Available online at www.sciencedirect.com
ScienceDirect
International Journal of Pharmaceutics 326 (2006) 160–168
INTERNATIONAL JOURNAL OF PHARMACEUTICS
www.elsevier.com/locate/ijpharm

Pharmaceutical Nanotechnology

Nanomolar cationic dendrimeric sulfadiazine as potential antitoxoplasmic agent

M.J. Prieto [a], D. Bacigalupe [b], O. Pardini [c,d], J.I. Amalvy [c,d], C. Venturini [b], M.J. Morilla [a], E.L. Romero [a,*]

[a] *Laboratorio de Diseño de Estrategias de Targeting de Drogas (LDTD), Departamento de Ciencia y Tecnología, Universidad Nacional de Quilmes, Roque Saenz Peña 180, Bernal B1876BXD, Buenos Aires, Argentina*
[b] *Laboratorio de Inmunoparasitología, Facultad de Ciencias Veterinarias, Universidad Nacional de La Plata, 60 Entre 118 y 119, La Plata 1900, Buenos Aires, Argentina*
[c] *INIFTA, Instituto de Investigaciones Fisicoquímicas Teóricas y Aplicadas (CONICET, CIC, UNLP), Departamento de Química, Facultad de Ciencias Exactas, Universidad Nacional de La Plata, Diag. 113 y 64 CC 16 Suc. 4, La Plata 1900, Buenos Aires, Argentina*
[d] *CIDEPINT, Centro de Investigación y Desarrollo en Tecnología de Pinturas (CIC-CONICET), Av. 52 Entre 121 y 122, La Plata 1900, Buenos Aires, Argentina*

Received 30 January 2006; received in revised form 25 April 2006; accepted 28 May 2006
Available online 1 July 2006

Abstract

The high doses of sulfadiazine (SDZ), used in synergistic combination with pyrimethamine, are mainly responsible for severe side effects and discontinuation of toxoplasmosis treatments. In the search for new strategies that improve the efficacy of treatments with reduced doses of SDZ, we have determined the performance of cationic G4 (DG4) and anionic G4.5 (DG4.5) poly(amidoamine) (PAMAM) dendrimers to act as SDZ nanocarriers. Both dendrimers could efficiently load SDZ (SDZ–DG4 and SDZ–DG4.5) up to a ratio of 30 molecules SDZ per dendrimer molecule. The MTT assay on Vero and J774 cells showed no cytotoxicity for DG4.5 and its SDZ complex incubated between 0.03 and 33 μM of dendrimer concentration. On the other hand, DG4 and its SDZ complex resulted cytotoxic when incubated at dendrimer concentrations higher than 3.3 μM. Finally, complexes and empty dendrimers were *in vitro* tested against Vero cells infected with RH strain of *Toxoplasma gondii* along 4 h of treatment. For SDZ–DG4.5 and DG4.5 to cause an infection decrease between 25 and 40%, respectively, a dendrimer concentration of 33 μM was required; however, SDZ–DG4 produced the highest infection decrease of 60% at 0.03 μM. These preliminary results, achieved with nanomolar doses of SDZ–DG4 as unique active principle, point to this complex as a suitable potential candidate for antitoxoplasmic therapy.

Keywords: Dendrimers; Sulfadiazine; Toxoplasmosis

1. Introduction

Difficulties for accession to intracellular targets enclosed within complex structural barriers, such as tachyzoites and bradyzoites of apicomplex parasite *Toxoplasma gondii*, require of active principles (AP) capable of crossing cell membranes or cell walls. However, there is only a few numbers of molecules with a suitable therapeutic activity against intracellular forms, since accession ability is harnessed by their own chemical structure (Samuel et al., 2003). Because of this, the strategy of loading an AP in a nanocarrier could be suitable to amplify their portfolio. Once loaded in a nanocarrier, constraints on molecular structure of AP to cross barriers can be disregarded. However, nano-structured nanocarriers (plain, ultradeformable, stealth, pH sensitive liposomes, immunoliposomes, nanoparticles, dendrimers) must then be carefully designed and/or chosen because pharmacokinetics, biodistribution, and selectivity for a tissue, cell group or intracellular compartments will exclusively depend on nanocarrier's structure. In designing a treatment against toxoplasmosis, when considering the complex microenvironment where tachyzoites and later bradyzoites reside (Samuel et al., 2003; Schatten and Ris, 2004), those nanocarriers capable of entering the cells by different (and perhaps more aggressive) mechanisms beyond the classical entrance modalities of lipo-

* Corresponding author. Tel.: +54 1143657100; fax: +54 1143657132.
E-mail address: elromero@unq.edu.ar (E.L. Romero).

0378-5173/$ – see front matter © 2006 Elsevier B.V. All rights reserved.
doi:10.1016/j.ijpharm.2006.05.068

somes and nanoparticles (phagocytosis and endocytosis, respectively) should deserve more attention. In this sense, dendrimers are exceptional polymers, with important advantages as compared to conventional linear or branched ones, such as absence of *entanglement* or sticky interactions (Uppuluri et al., 1998, 2000) monodisperisty (Bosch and Corrales, 2003), controlled size in the range of nanometers units, controlled number of surface groups and extremely high area/volumen ratio in comparison with other nanocarriers. Only intermediate generation (G) dendrimers (3.5–5G) are suitable drug carriers, with structure open enough to enable the loading and subsequent release of molecules in a controlled fashion (Mallamace et al., 2002; Canetta and Maino, 2004; Han et al., 2005).

Adsorption to and disruption of plasma membrane, and the endosomolysis when captured by endocytosis, are special features of cationic PAMAM dendrimers. Cationic dendrimers can establish three union points with cell membranes (Fischer et al., 2003) needed to elicit biological responses, because of their tridimentional structure and flexibility. Branched and flexible dendrimers of high charge densities can more efficiently interact with cell surface than rigid globular or linear polymers, to cause structural changes on lipid membranes (Zhang and Smith, 2000). Finally, cationic PAMAM dendrimers are weak bases capable of protonate the tertiary amines of their branching points (6.85 pK_a) (Tajarobi et al., 2001) under physiologic pH. If captured by endocytosis, cationic PAMAM dendrimers inside the endosomes act as buffers, inducing the uptake of protons that conduces to osmotic imbalance and lysis of endosomes (Aulenta et al., 2003). This endosomolytic effect is an important mechanism that mediates the dendrimers access to cell cytoplasm.

Membrane superposition and fusion mediate the entrance of dendrimers across lipid bilayers and there is abundant experimental evidence on their capability to generate holes in the surface of liposomes and cell membranes (Karoonuthaisiri et al., 2003; Hong et al., 2004; Mecke et al., 2004; Yang et al., 2005). This singular entrance modality of dendrimers be probably of help to offer massive or efficient delivery of AP to intracellular targets. Toxoplasmic encephalitis is a life threatening form of the disease caused by cyst reactivation. The current medication based on synergistic combination of sulfadiazine (SDZ)/pyrimethamine requires of high amounts of SDZ and causes severe side effects (Couvreur et al., 1991; Araujo et al., 1993; Djurkovic-Djakovic et al., 2000; Petersen et al., 2001). Hence, developing a nanocarrier for more efficient delivery of SDZ to intracellular targets, should not only reduce those high doses, but could also improve efficacy and reduce the extent of treatments. In this work we will explore the performance of dendrimers as SDZ nanocarriers against an *in vitro* model of cells infected with tachyzoites of *T. gondii*.

2. Materials and methods

2.1. Materials

Poly(amidoamine) (PAMAM) dendrimer G4 (PAMAM–G4–NH_2) (molecular weight = 14,215 g/mol, 64 amine end groups) (DG4) and PAMAM–G4.5–COOH (molecular weight = 26,258 g/mol, 128 carboxylate end groups) (DG4.5) were purchased from Sigma–Aldrich, Argentina. Sulfadiazine (SDZ) 99.0%, fluorescein isothiocyanate isomer I (FITC), sodium 3-(4,5-dimethythiazole-2-yl)-2,5-diphenyltetrazolium bromide (MTT) and benzoylated dialysis membrane were also from Sigma–Aldrich Argentina. RPMI 1640 culture medium was purchased from Invitrogen Corporation. Calf bovine serum was from Bioser Gen SA, Argentina. L-Glutamine, Trypsin, EDTA and Penicillin/Streptomycin were provided by PAA Laboratories GmbH, Austria. Tris buffer and all the other reactive used were analytical grade from Anedra, Argentina.

2.2. Drug complex to dendrimers

Different amounts of DG4 and DG4.5 were combined with SDZ in methanolic solution at different SDZ:dendrimers (D) molar ratios (20, 35, 47, 70 and 140); corresponding to 6 mM of SDZ and 280, 168, 118, 87 and 44 μM of D, respectively. The mixtures were incubated for 45 h at room temperature (20 °C) and methanol evaporated in a Speed Vac at (25 °C) (1010 SAVANT). The solid residues obtained were dissolved in 0.1 ml of Tris buffer 10 mM pH 7.5 plus NaCl 0.9% p/v (Tris buffer) at room temperature and centrifuged at 10,000 × *g* for 5 min, in order to separate the SDZ–dendrimer (SDZ–D) complexes (soluble SDZ) from the non incorporated SDZ (insoluble). Additionally, DG4 and SDZ were combined in alkaline medium (pH 11, adjusted with NaOH 1 M) at 70, 140, 280 and 580, SDZ:D molar ratios. Upon incubation the aqueous medium was evaporated and solid residues were dissolved in Tris buffer and SDZ–D complexes separated as state above.

2.3. SDZ quantification

The amount of SDZ complex to dendrimers was quantified by measuring absorbance at 255 nm with UV–vis Shimadzu spectrophotometer UV-160 A. Dendrimers do not absorb at this wavelength. The calibration curve of SDZ in Tris buffer was linear in a concentration range of 1–5 μg ml^{-1} ($r^2 = 0.99$). On the other hand, FT-IR spectroscopy showed no remnant dendrimers in the insoluble residue obtained after centrifugation as absence of peak at 1557 cm^{-1}, therefore complete dissolution of dendrimers into the complexes was assumed.

2.4. Characterization of SDZ–D complexes

FT-IR spectra of SDZ, dendrimers and SDZ–D complexes were measured using a Perkin Elmer Spectrum One spectrometer. Samples were prepared by evaporation of 20 μl of Tris buffer solutions (33 μM of dendrimers) at 30 °C on a CaF_2 window. Corrections for the CaF_2 window absorption at low wave numbers were made accordingly. For SDZ (powder-like sample), an universal ATR accessory was used. The number of scan in all cases per experiment was 64.

2.5. In vitro release studies

In vitro release of SDZ from SDZ–D complexes was investigated in Tris buffer using dialysis bag diffusion technique. SDZ–D complexes were sealed in benzoylated dialysis bag (Mw cut-off: 2000) and incubated in Tris buffer under continuous stirring. SDZ released into the incubation medium was collected at pre-determined time intervals and stored for quantitative analysis. The amount of SDZ released was determined by absorbance at 255 nm as described in Section 2.3.

2.6. Cytotoxicity assay

Cell viability upon treatment with SDZ, dendrimers and SDZ–D complexes, measured as mitochondrial succinate dehydrogenase activity employing a tetrazolium salt (MTT), was determined on Vero cells and on the murine macrophage-like cell line J774. Cells were maintained at 37 °C in RPMI-1640 medium supplemented with 10% heat-inactivated foetal calf serum, 100 UI/ml penicillin and 100 μg/ml streptomycin in an atmosphere of 5% CO_2. Cells were seeded at a density of 5×10^4 cells/well in 96-well flat bottom microplates. After 24 h, the culture medium was replaced by 100 μl of 10-fold-serial dilutions of SDZ (1–1×10^{-4} mM), dendrimers (33–0.03 μM), or SDZ–D complexes (1–1×10^{-3} mM SDZ and 33–0.03 μM D). Upon 24 h or 4 h incubation (only for SDZ–D complexes at 1 mM SDZ–33 μM D), solutions were removed and replaced by fresh RPMI medium and MTT at 0.5 mg ml^{-1} final concentration. After 3 h incubation, MTT solution was removed, the insoluble formazan crystals were dissolved in dimethylsulfoxide (DMSO) and absorbance was measured at 570 nm using a microplate reader.

2.7. Cell internalization

Dendrimers and SDZ–D complexes were labelled with FITC according to Kolhe (Kolhe et al., 2003). Briefly, buffer solutions of D or SDZ–D were incubated with FITC acetonic solution at a 1:20, D:FITC molar ratio, in the dark at room temperature. Upon overnight incubation, non-incorporated FITC was eliminated by dialysis against Tris buffer and the remnant solvent in the bag was evaporated. The solid residue was dissolved with Tris buffer and degree of FITC labelling was estimated by correlating the absorbance of FITC labelled dendrimers in Tris buffer at 492 nm with a previously prepared calibration curve between 1.6 and 8 μg FITC ml^{-1}.

Vero cells were seeded in three 24-well plates with rounded coverslips on the bottom; after 48 h incubation the medium was removed and submitted to different treatments. Two plates were incubated with FITC–D solution (0.33 μM D), one at 37 °C and the other at 4 °C. Upon 4 h incubation, cells were washed with phosphate-buffer saline (pH 7.4) (PBS), fixed with methanol for 10 min and the emission of FITC monitored with an Olympus BH-RFGA fluorescence microscope. The third plate was incubated with FITC–D or FITC–SDZ–D (1 mM SDZ–33 μM D) at 37 °C, supernatant were removed at 0, 1 and 4 h and the amount of FITC was quantified by calibration curve recorded at 492 nm.

2.8. Anti-toxoplasmic activity of SDZ–D complexes

Vero cells maintained as described above were seeded in 24-well plates with rounded coverslips on the bottom. After 48 h incubation, cells were infected with *T. gondii* tachyzoites, RH strain, at a cell–parasite ratio of 2:1 for 2 h. After 48 h cells were treated with SDZ (1 mM), dendrimers at two concentration levels (33 and 0.03 μM) or SDZ–D complexes at both concentration levels (1 mM SDZ–33 μM D and 1×10^{-3} mM SDZ–0.03 μM D) for 4 h at 37 °C. Cells were washed and further incubated 48 h in fresh medium at 37 °C. The coverslips were removed, washed with PBS, fixed with methanol and stained with Giemsa. Both number and size of infection foci, as well as number and magnitude of cell burst were determined by light microscopy. Arbitrary values between 1 and 3 were assigned to focus size and magnitude of cell burst as follows: focus size = 3 if mean diameter > 2 arbitrary length units; 2 if mean diameter = 2 arbitrary length units and 1 if mean diameter = 1 arbitrary length units; *magnitude of cell burst,* determined as size of cleared area, was calculated following the same criteria for assignments used for classifying the foci size. Foci and burst ponder media was calculated as the sum of all values and dividing by foci or burst number. Untreated infected cells were used as control.

2.9. Calculations

Infection decrease (ID) was calculated as: ID = 100 − [TE × (100)/(control)], where treatment effect (TE) was calculated as: TE = (ponder media of foci size) × (foci number) × (ponder media of burst magnitude) × (cell burst number).

3. Results

3.1. SDZ complex to dendrimers

Complex formation ability of full and half generation PAMAM dendrimers (DG4 and DG4.5) were assayed in two media where SDZ was completely dissolved (its crystalline lattice disrupted), to select the best medium in terms of maximize the number of SDZ molecules incorporated to dendrimer molecule. To that aim, SDZ and dendrimers were co-solubilized in methanol or alkaline medium (pH 11) and incubated in different molar ratios.

When incubated in alkaline medium, although higher amounts of SDZ were offered to dendrimers, SDZ was not efficiently complexed, resulting less than 1 molecule of SDZ per dendrimer.

When incubated in methanol, however, combination molar ratios lower than 35:1 (SDZ:D) rendered complexes of crescent ratios up to a maximum of 30:1. At that point dendrimer saturation was achieved, and higher combination ratios did not produce higher amounts of SDZ complexed (Fig. 1)

Solubility of SDZ increased linearly ($r^2 = 0.96$) with increasing concentration of DG4 and DG4.5 as shown in Fig. 2. The corresponding slops of linear regressions were 33.8 for DG4 and 28.6 for DG4.5, which was coincident with the average of SDZ molecules complexed by both dendrimers. Hence, upon

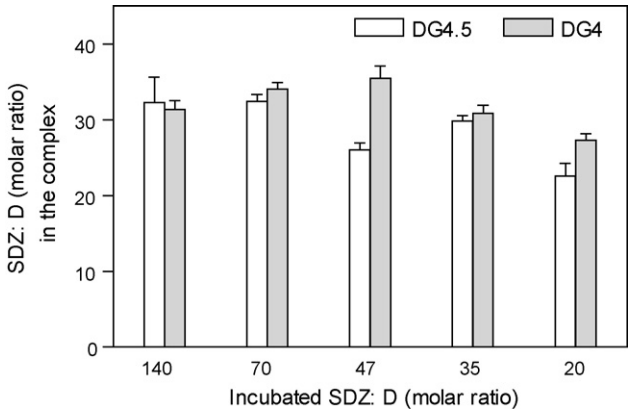

Fig. 1. SDZ incorporation into G4 and G4.5 dedrimers as function of incubated SDZ:dendrimer, molar ratio in methanol ($n = 6$). Quantity of SDZ complex was corrected by SDZ solubility in tris buffer (1.17 mg ml^{-1}).

complexation, the new aqueous solubility of SDZ, expressed as molar concentration, can be roughly calculated as 30 multiplied by dendrimer concentration.

3.2. Characterization of SDZ–D complexes

FT-IR spectrum of solid SDZ (Fig. 3a) showed the amine ($-NH_2$) stretching bands at 3420 and 3350 cm^{-1}, with N–H stretching of sulfonamide at 3260 cm^{-1} and its corresponding bending band at 1652 cm^{-1}. The sulfone moiety bands were observed at 1326 and 1157 cm^{-1} (Brandmuller and Wahl, 1967; Garcia-Raso et al., 2000).

On the other hand, bending corresponding to primary amine groups at 1644 cm^{-1}, stretching of C–H bonds inside the core at 1557 cm^{-1}, and N–H stretching at 3286 cm^{-1} are shown in DG4 FT-IR spectrum (Fig. 3b) (Kolhe et al., 2003).

For SDZ–DG4 complex, broaden and shifted stretching N–H peak (3345 cm^{-1}) was strong evidence of the presence of NH_3^+ (Fig. 3c) (Asthana et al., 2005), indicating possible electrostatic association of SDZ with dendrimer. Electrostatic interactions could be established between the positively charged primary amines of PAMAM DG4 (pKa between 7 and 9) and negatively

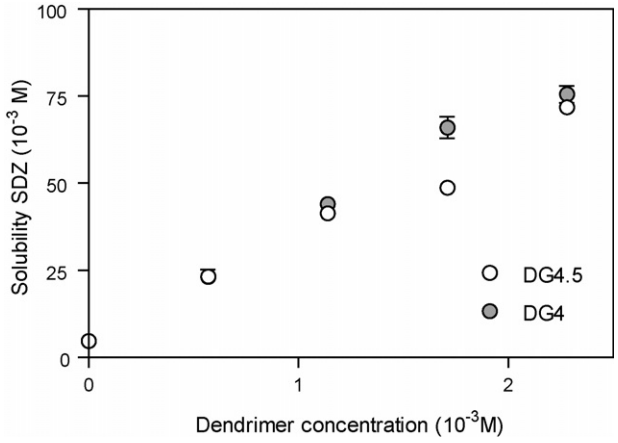

Fig. 2. Solubility profile of SDZ as function of increasing concentration of DG4 and DG4.5 in Tris buffer ($n = 3$).

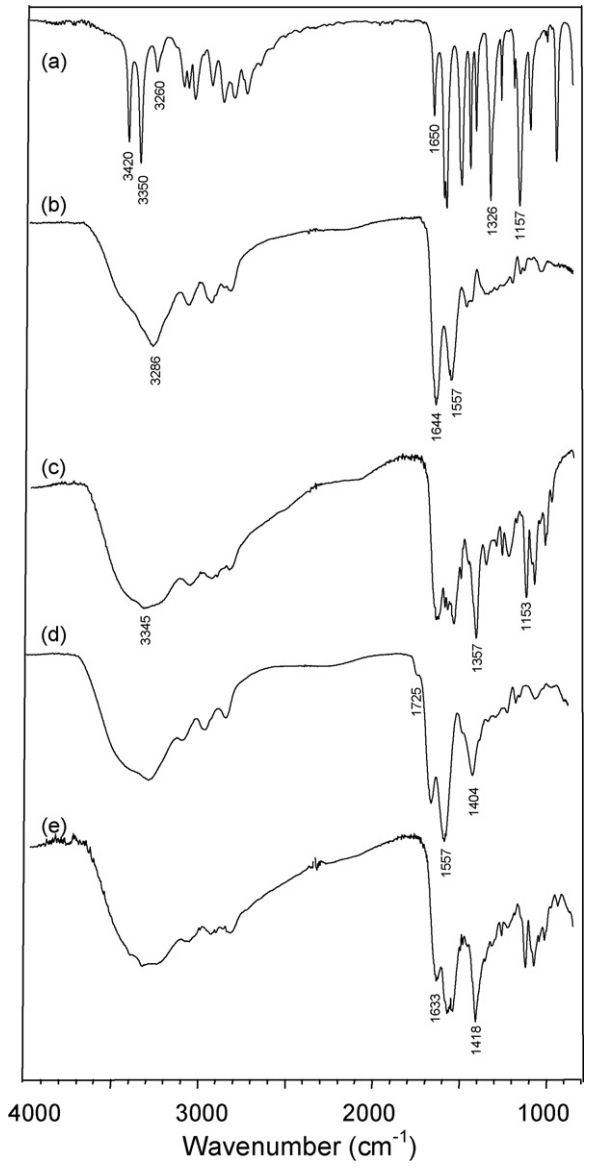

Fig. 3. FT-IR spectrums of: (a) SDZ, (b) DG4, (c) SDZ–DG4 complex, (d) DG4.5 and (e) SDZ–DG4.5 complex.

charged SDZ (a weak acid with pK_a of 6.4) at pH 7.5. According to this, in Tris buffer at pH 7.5 almost all SDZ is in its anionic form while most of the 64 surface amino groups of each DG4 molecule are ionized enabling electrostatic interactions.

FT-IR of DG4.5 (Fig. 3d) showed a band at 1725 cm^{-1} corresponding to the vibrational C=O stretching of the carboxylic terminal groups and a strong band due to symmetric vibrational stretching of deprotonated carboxylate groups at 1404 cm^{-1} (Coates, 2000; Endo et al., 2005). Also, it showed the same stretching of C–H bonds inside the core at 1557 cm^{-1} than DG4.

For SDZ–DG4.5 complex (Fig. 3e), several changes and new bands appeared in the spectrum but the most interesting feature was the disappearance of the carbonyl band at 1723 cm^{-1} and the shift of the carboxylate band at 1418 cm^{-1}. Also a new band at 1633 cm^{-1} appeared, probably due to the bending mode of SDZ–NH_2 group. Half generation dendrimers (DG4.5) have only tertiary amines in their internal cavities, which are less sus-

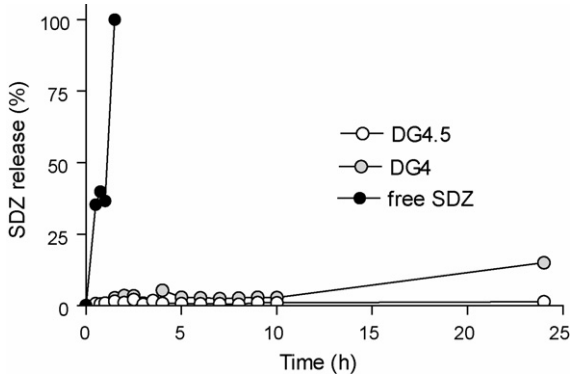

Fig. 4. Release profiles of SDZ from SDZ–D complex in Tris buffer.

ceptible to protonation than primary amines. At pH 7.5 these dendrimers are not positively charged and can not interact electrostatically with the drug molecules. In this case the interaction was expected to be due H-bond between the $–NH_2$ and carboxylic groups.

3.3. In vitro release

The strength and stability of drug–dendrimer complexes was examined by determining the *in vitro* release of SDZ against Tris buffer. Fig. 4 showed that almost 100% of free SDZ was released in 90 min, but SDZ–DG4.5 complex retained around 98% of SDZ along 24 h, while SDZ–DG4 retained around 85%. These results were consistent with that of Kolhe et al. (2003), where less than 15% of the acidic drug ibuprofen being released from its PAMAM–G4 complex in deionized water after 9h. Hence, both SDZ–D complexes resulted structurally stable in buffer.

3.4. Cytotoxicity

The effect of dendrimers, SDZ and SDZ–D complexes on viability of two cell types, was measured by the MTT assay.

SDZ did no reduce viability on Vero or J774 cells upon 24 h incubation over the tested concentration range ($1–1 \times 10^{-4}$ mM) (data not shown).

DG4.5 at concentrations between 0.03 and 33 μM, did not reduce the viability of Vero or J774 cells upon 24 h incubation, whereas DG4 significantly decreased the viability of both cell types at concentrations at or above 3.3 μM (Fig. 5a and b). With respect to the complexes, SDZ–DG4.5 between 0.03 and 33 μM (D concentration) did not reduce the viability of Vero or J774 cells upon 24 h incubation, whereas SDZ–DG4 decreased the viability of both cell types at concentrations at or above 3.3 μM (Fig. 5a and b).

The effect of DG4 and SDZ–DG4 complex on viability was more pronounced on J774 than on Vero cells, being 40 and 70%, respectively at 3.3 μM (D concentration) and falling to 2 and 20% at 33 μM (D concentration). After shorter incubation times of 4 h, no cytotoxic effect on J774 or Vero cells was detected even at maximal concentration of DG4, DG4.5 and SDZ–DG4.5 complex; however, significant reduction of viability was caused by 33 μM of the SDZ–DG4 complex (Fig. 5c and d).

3.5. Cell internalization

FITC-labelled dendrimers were used to assess the relative contribution of adsorption and internalisation by Vero cells, using a combination of fluorescence microscopy and UV–vis spectroscopy. FITC labelling of dendrimers resulted an average of 4 molecules of FITC per DG4 or SDZ–G4 molecule and 11 molecules of FITC per DG4.5 or SDZ–DG4.5 molecule.

Fluorescence images of Vero cells incubated 4 h with FITC-labeled dendrimers either at 37 or 4 °C (temperature at which internalisation by endocytic uptake is absent due to reduced metabolism of cells), are showed in Fig. 6. Upon incubation at 37 °C both dendrimers were captured and entered the cells, as seen by the characteristic endocytic spots, while at 4 °C, a general decrease in fluorescence was recorded. The level of fluorescence intensity showed in Fig. 6e, revealed that internalisation of FTIC–DG4 at 37 °C was 6 folds higher than that of FITC–DG4.5, whereas at 4 °C only FITC–DG4 was capable of being adsorbed onto plasma membranes.

On the other hand, the fluorescence intensity at 37 °C (endocytic uptake) for FITC–DG4 resulted to be slightly minor than that at 4 °C (adsorption). As seen by the contribution of this last relatively high intensity, the interaction with cells of FITC–DG4 probably was the resultant of two processes: adsorption and endocytic uptake. At the experience concentration (0.33 μM), no differences between uptake of dendrimers or their respective SDZ complexes were found (data not shown).

Absorbance of supernatants from Vero cells incubated with 33 μM FITC-labelled dendrimers was recorded as a function of time. As shown in Fig. 7, decreased of FITC concentration in supernatant occurred at maximal rate during the first hour, to decrease at longer times for FITC–DG4, FITC–DG4.5 and FITC–SDZ–DG4.5. These results can account for internalisation of FITC-labelled dendrimes into cells.

Percentage of dendrimer internalization calculated from FITC concentration in supernatants and obtained FITC:D molar ratio showed that FITC–DG4.5 was internalized twice folds as compared to FITC–SDZ–DG4.5, upon 4h incubation.

3.6. In vitro antiparasitic effect

SDZ 1 mM had no antiparasitic effect, neither as DG4.5, SDZ–DG4.5 nor DG4 at 0.03 μM, DG4 and SDZ–DG4 strongly reduced the viability of host cells at 33 μM. Antiparasitic activity was found for DG4.5 (40% infection decrease) and for SDZ–DG4.5 (25% infection decrease) both at 33 μM. SDZ–DG4 however, showed maximal antiparasitic effect at 0.03 μM (60% infection decrease). Note that the antiparasitic effect reported above, is an arbitrary number (see Fig. 8) calculated with the only aim of establishing an intra-assay comparison between each treatment, not of use to be contrasted against real data on tachyzoites/bradyzoites development obtained by conventional methods (Derouin and Chastang, 1988; Roos et al., 1994; Mc Fadden et al., 1997).

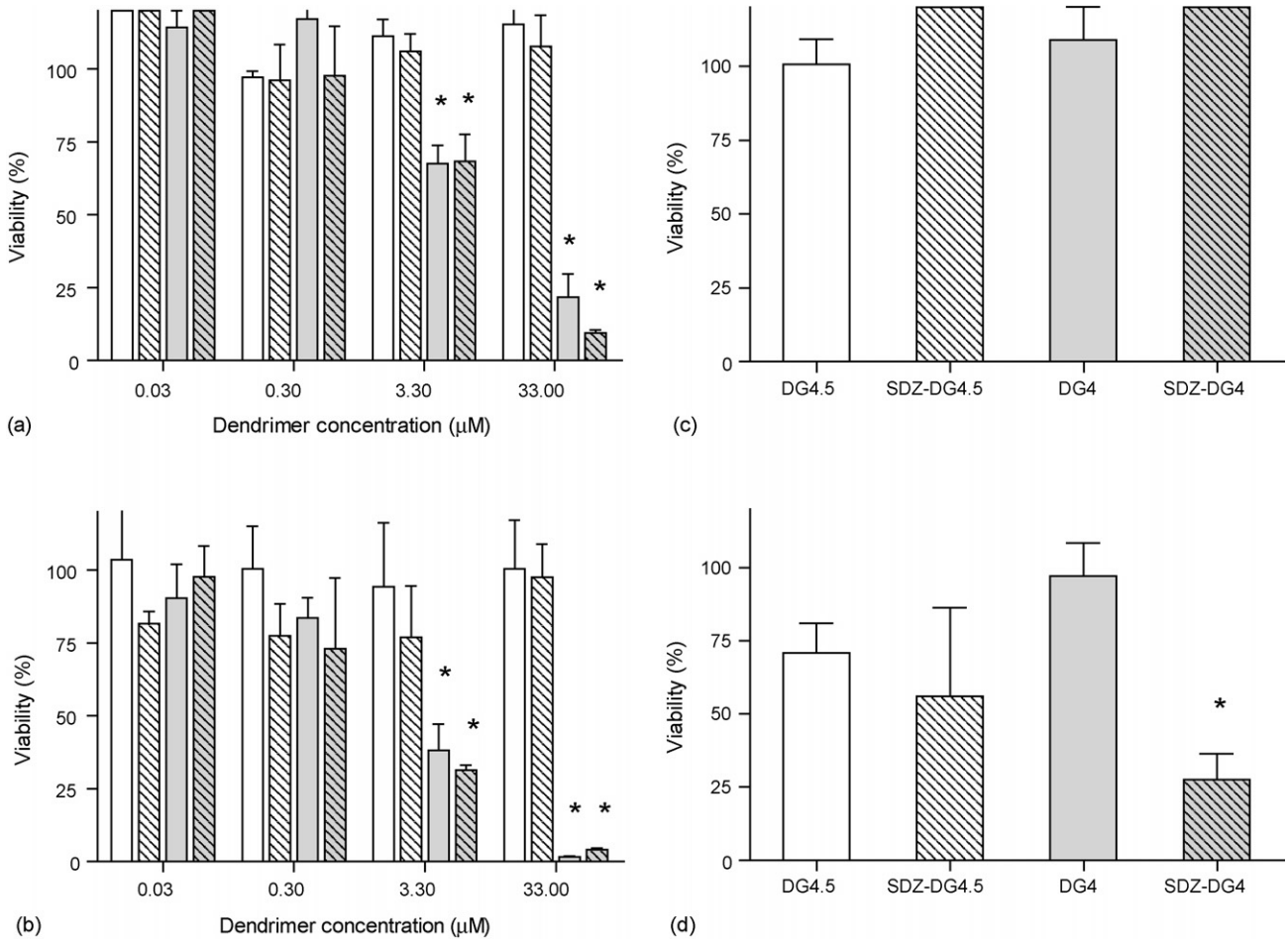

Fig. 5. Dose-dependent cytotoxicities of dendrimers ((□) DG4.5; (▨) DG4) and SDZ–D complex ((▧) SDZ–DG4.5; (▨) SDZ–DG4) after 24 h incubation on Vero (a) and J774 cells (b). Cytotoxicity of 33 μM of dendrimers after 4 h on Vero (c) and J774 cells (d). Each data point represents the mean ± standard deviation ($n = 3$). Student's t-test was used to compare statistical significance of treatments (differences: * $p < 0.05$).

4. Discussion

In this work, we have shown that when prepared from mixtures co-dissolved in methanol, PAMAM G4 and G4.5 formed stable and efficient complexes with SDZ, a poorly hydrosoluble drug at physiological pH. Co-dissolution of drug and DG4 in alkaline media, was an unsuitable strategy to render complexes of high drug payload upon rehydration. The effect of pH on stability of SDZ must be considered in terms of net charge of its sulfanamide moiety ($pK_a = 6.4$). At pH 11, SDZ exhibits its higher solubility, being 100% in its ionized (negatively charged) form. With regard to DG4, at high pH none of the primary or tertiary amines are protonated, and an increased translational and rotational diffusion of water molecules, with a less rigid backbone because of the neutralized internal charges, are registered. In general terms, changes of pH mainly modify the DG4 ionization degree; therefore, conformational transformations are induced (Tai et al., 2005). Structural changes in cationic PAMAM dendrimers, analyzed as function of pH and D generation, showed the D as globular and loosely compact structures at high pH (≥10), with conservation of atom density distribution across generations (Inhan et al., 2002; Cakara et al., 2003). Finally, the work of Bharathi (Bharathi et al., 2005), found that the interaction of a weak acid drug completely ionized at pH 11 and possessing maximal solubility with PAMAM dendrimers, is minimal in extreme alkaline medium. Taken together, those facts offer a simple explanation for the unsatisfactory complexation of SDZ in DG4 when co-dissolved in alkaline medium: at high pH – in spite of achieving maximal SDZ solubility – the structure of PAMAM dendrimer was collapsed, and therefore drug access to the internal pockets resulted impaired.

Hence, the complexation in methanol resulted a simple way of increasing aqueous solubility of SDZ up to a maximal of 30 multiplied by dendrimer concentration, without any chemical modification of drug structure. Both complexes shared common features, such as drug:D molar ratio and degree of release against dilution. Their FT-IR spectra however, showed that electrostatic attraction mediated the SDZ–DG4 interaction, whereas in SDZ–DG4.5 presented hydrogen bonding as the main interaction. The uptake of dendrimer complexes was studied on two cell lines possessing different entrance mechanisms: only endocytic (Vero cells) and endo/phagocytic the other (J774 cells). MTT assay showed that neither DG4.5 not its corresponding SDZ complex decreased cell viability of Vero and J774 cells in the tested range of concentration; DG4 and its SDZ complex on the other hand, were cytotoxic at the micromolar range.

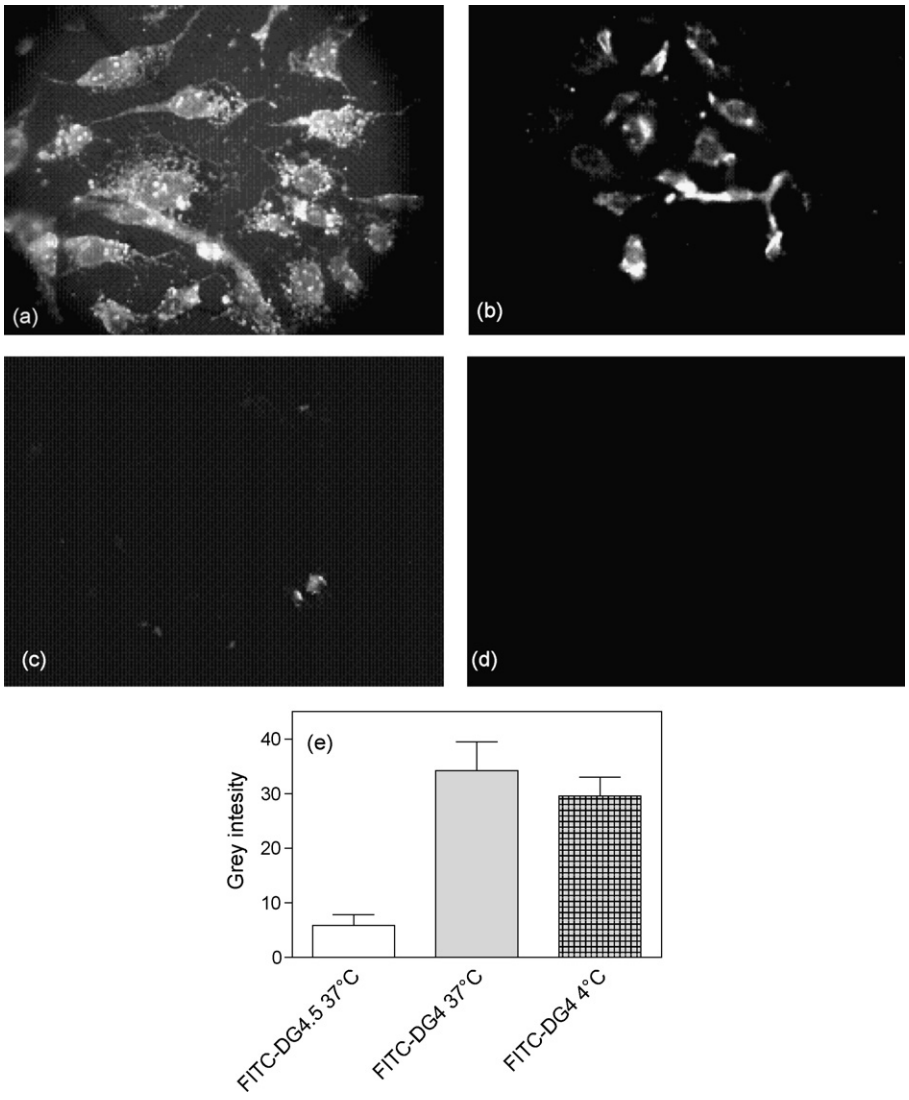

Fig. 6. Fluorescence microscopy images of Vero cells upon incubation with FITC–DG4 at 37 °C (a) and 4 °C (b), and with FITC–DG4.5 at 37 °C (c) and 4 °C (d). (e) Quantification of dendrimer entry, intensity of cells was determinate using ImageJ imaging software.

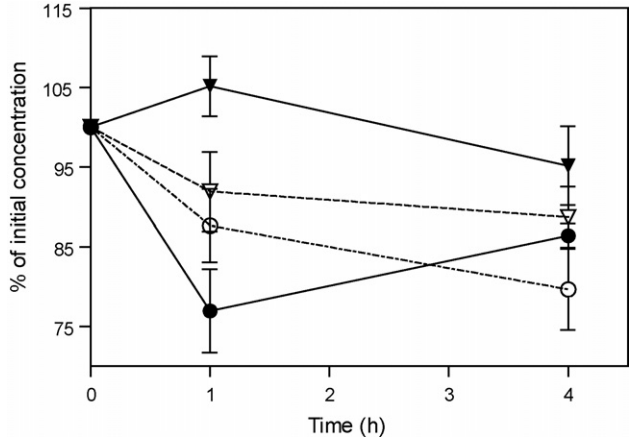

Fig. 7. FITC concentration in Vero cell supernatant (from absorbance) as function of incubation time of: (–●–) FITC–DG4; (···⊖···) FITC–DG4.5; (–▼–) FITC–SDZ–DG4; (···▽···) FITC–SDZ–DG4.5. Each data point represented the mean ± standard deviation ($n = 3$).

The most striking feature of SDZ–DG4 was revealed, however, when *in vitro* tested against Vero cells infected with a RH strain of *T. gondii*. Our results pointed to SDZ–DG4 as responsible for the highest antiparasitic effect, in spite of being administered at ultra low doses – in the range of nanomolar concentration – and upon only 4 h of treatment. It was also found that SDZ–DG4.5 had low antiparasitic effect and surprisingly, that DG4.5 had got antiparasitic effect on its own.

The uptake assays at 37 °C versus 4 °C showed that only DG4 interacted with plasma membrane by a mechanism other than endocytosis. This is coincident with the observations performed by atomic force microscopy on the interaction between cationic PAMAM G5 dendrimers and supported bilayers, showing that low generation dendrimers can remove lipids from the borders of pre-existent defects and that at 6 °C cationic PAMAM G5 adsorbs on plasma membrane, without releasing cytoplasmic enzymes (Hong et al., 2004). Hence the combination of surfacial activity and endosomolytic effect could be at least in part responsible for the antiparasitic effect of SDZ–DG4 at

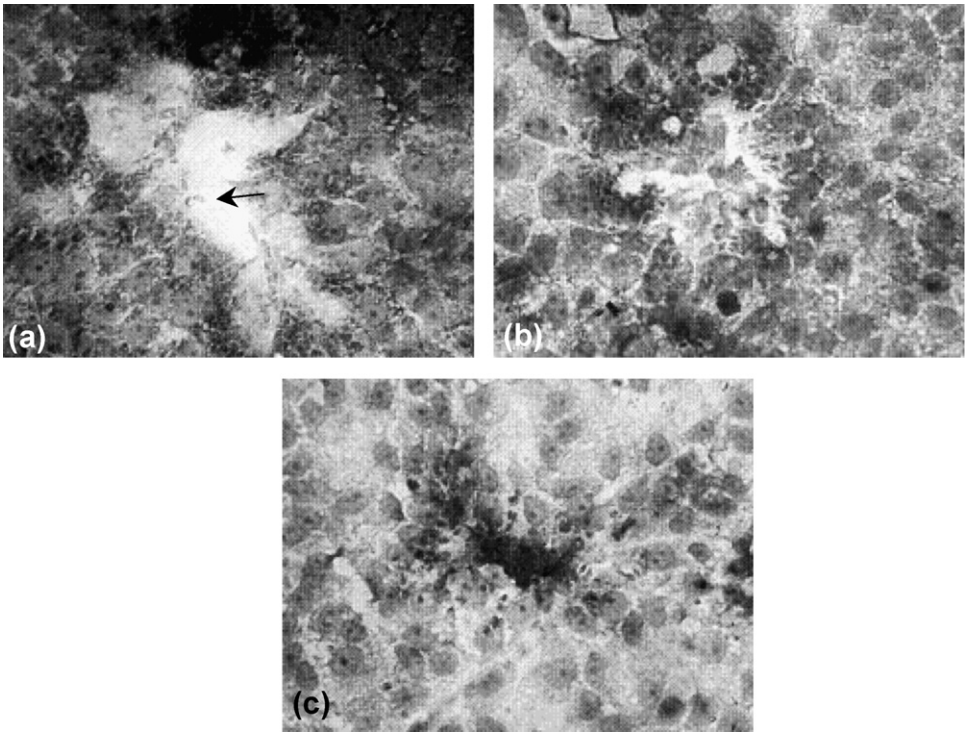

Fig. 8. Representative images of infected cultures employed to calculate the anti-toxoplasmic activity of treatments: (a) big focus and big cell burst, arrow show a parasite; (b) medium size focus and medium size cell burst; (c) small focus, absence of cell burst.

the ultra-low concentration of 0.03 μM, which is one thousand folds lower than that of SDZ–DG4.5 presenting anti-infective activity. SDZ–DG4 on the other hand, contained 1×10^{-3} mM SDZ (250 ng ml^{-1}), being this concentration 1×10^{9} lower than *in vitro* IC50 for SDZ, 2.5 g ml^{-1}, determined upon 72 h on infected MRC5 fibroblasts (Duval and Leport, 2001). As seen in Fig. 6a, FITC–SDZ–DG4 at 33 μM mostly remained outside the cells during the four hours of incubation; however, it was known to be cytotoxic at that concentration. Hence, FITC–SDZ–DG4 caused cell death by mechanisms that did not depend on dendrimer uptake, most probably related to damages on surface membrane.

Probably in the absence of plasma membrane interaction and endosomolytic effect, DG4.5 and SDZ–DG4.5 were endocytosed and degraded by the endo-lysosomal route. If not delivered to the cytoplasm, dendrimers should not have access to the therapeutic target, this is the parasitophorous vacuole. This should only account for the lower anti-infective performance of SDZ–DG4.5 as compared to SDZ–DG4, but we have no current explanation for the anti-infective effect displayed by DG4.5. The intracellular pathway and metabolisation of DG4, DG4.5 and their respective SDZ complexes however, remains to be elucidated, both in healthy and very importantly, on infected cells. The profound structural changes that both plasma membrane and cytoplasm of host cell suffer when infected with *T. gondii* tachyzoites could have a role in the antiparasitic activity found for DG4.5. There is a new great complexity inside the infected cells: tachyzoites surround by a PV, with membrane channels that acting as molecular sieves, impair the entrance of molecules with MW higher than 1.4 KD (Schwab et al., 1994). The PV remains isolated from the lysosomal and vesicle trafficking system of the host cell (Sinai et al., 1997; Saliba and Kiaran, 2001; Coppin et al., 2003). There is also an intravacuolar tubulovesicular netwok, which appears to be continuous with the tachyzoites's plasma membrane (TPM) (with endocytic mechanisms localised to a micropore (Nichols et al., 1994; Robibaro et al., 2001), and transporters related with nutrients acquisition) that forms connections with the parasitophorous vacuole membrane (PVM) (Zhang et al., 2001). The existence of these elaborated connections can strongly alter the intracellular processing of the nanocarriers and further studies will be required to shed light on this important topic. SDZ inhibits the enzyme dihydropteroate synthase and together with pyrimethamine, synergistically blocks the nucleotide pathway of the parasite. Unfortunately, adverse events-mostly fever related to the high doses of SDZ-frequently result in discontinuation of therapy. Our *in vitro* preliminary results, achieved with nanomolar doses of dendrimeric SDZ as unique active principle, point to this complex as a suitable potential candidate for antitoxoplasmic therapy.

Acknowledgements

This research was supported by a grant from Secretaría de Investigaciones Universidad Nacional de Quilmes M.J. Morilla and E.L. Romero are members of the Carrera de Investigador Científico Consejo Nacional de Investigaciones Científicas y Técnicas (CONICET, Argentina). J.I. Amalvy is Member of Comisión de Investigaciones Científicas de la Provincia de Buenos Aires, (CICPBA) Argentina. M.J. Prieto has got a fellowship from CONICET, Argentina.

References

Araujo, F.G., Lin, T., Remington, J.S., 1993. The activity of atovaquone (566C80) in murine toxoplasmosis is markedly augmented when used in combination with pyrimethamine or sulfadiazine. J. Infect. Dis. 167 (2), 494–497.

Asthana, A., Chauhan, A.S., Diwan, P.V., Jair, N.K., 2005. Poly(amidoamine) (PAMAM) dendritic nanostructures for controlled site-specific delivery of acidic anti-inflammatory active ingredients. AAPS Pharm. Sci. Technol. 6 (3), E536–E542.

Aulenta, F., Hayes, W., Rannard, S., 2003. Dendrimers: a new class of nanoscopic containers and delivery devices. Eur. Polym. J. 39, 1741–1771.

Bharathi, D., Hill, R.A., Liebenberg, W., Brits, M., de villiers, M.M., 2005. Comparison of the aqueous solubilization of practically insoluble niclosamide by polyamidoamine (PAMAM) dendrimers and cyclodextrins. Int. J. Pharm. 304, 193–209.

Bosch, P., Corrales, T., 2003. Polimeros dendríticos: propiedades y aplicaciones. Revista Plasticos Modernos 86 (567), 242–249.

Brandmuller, J., Wahl, M., 1967. Vibration-spectroscopic studies on the modus of antibacterial action of sulfonamides. Spectrochim. Acta Part A 23, 2465–2469.

Cakara, D., Kleimann, J., Borkovec, M., 2003. Microscopic protonation equilibria of poly(amidoamine) dendrimers from macroscopic titrations. Macromolecules 36, 4201–4207.

Canetta, E., Maino, G., 2004. Molecular dynamic analysis of the structure of dendrimers. Nucl. Instrum. Meth. Phys. Res. B 213, 71–74.

Coates, J., 2000. Interpretation of infrared spectra A practical approach. In: Meyers, R.A. (Ed.), Encyclopedia of Analytical Chemistry. John Wiley & Sons Ltd., Chichester, pp. 10815–10837.

Coppin, A., Dzierszinski, F.L., Mortuaire, S.M., Ferguson, D., Tomavo, S., 2003. Developmentally regulated biosynthesis of carbohydrate and storage polysaccharide during differentiation and tissue cyst formation in *Toxoplasma gondii*. Biochimie 85, 353–361.

Couvreur, J., Thulliez, P., Daffos, F., Aufrant, C., Bompard, Y., Gesquiere, A., Desmonts, G., 1991. Fetal toxoplasmosis. In utero treatment with pyrimethamine sulfamides. Arch. Fr. Pediatr. 48 (6), 397–403.

Derouin, F., Chastang, C., 1988. Enzyme immunoassay to assess effect of antimicrobial agents on *Toxopasma gondii* in tissue culture. Antimicrob. Agents Chemother. 32, 303–307.

Djurkovic-Djakovic, O., Roman, S., Nobre, R., Couvreur, J., Thulliez, P., 2000. Serologic rebounds after one-year-long treatment for congenital toxoplasmosis. Pediatr. Infect. Dis. J. 19 (1), 81–83.

Duval, X., Leport, C., 2001. Toxoplasmosis in AIDS. Curr. Treatment Options Infect. Dis. 3, 113–128.

Endo, T., Tomokazu, Y., Kunio, E., 2005. Synthesis and catalytic activity of gold–silver binary nanoparticles stabilized by PAMAM dendrimer. J. Colloid Interf. Sci. 286 (2), 602–609.

Fischer, D., Li, Y., Ahlemeyer, B., Kriegstein, J., Kissel, T., 2003. *In vitro* cytotoxicity testing of polycations: influence of polymer structure on cell viability and hemolysis. Biomaterials 24, 1121–1131.

Garcia-Raso, A., Fiol, J.J., Rigo, S., Lopez-Lopez, A., Molins, E., Espinosa, E., Borras, E., Alzuet, G., Borras, J., Castineiras, A., 2000. Polyhedron 19, 991–997.

Han, M., Chen, P., Yang, X., 2005. Molecular dynamics simulation of PAMAM dendrimer in aqueous solution. Polymer 46, 3481–3488.

Hong, S., Bielinska, A.U., Mecke, A., Keszler, B., Velas, J.L., Shi, X., Balogh, L., Orr, B.G., Baker, J.R., Banaszak Holl, M.M., 2004. Interaction of poly(amidoamine) dendrimers with supported lipid bilayers and cells: hole formation and the relation to transport. Bioconjugate Chem. 15, 774–782.

Inhan, L., Athey, B.D., Wetzel, A.W., Meixner, N., Baker Jr., J.B., 2002. Structural molecular dynamics studies on polyamidoamine dendrimers for a therapeutic application: effects of pH and generation. Macromolecules 35, 4510–4520.

Karoonuthaisiri, N., Titiyevskiy, K., Thomas, J.L., 2003. Destabilization of fatty acid-conaining liposomes by polyamidoamine dendrimers. Colloid Surf. B: Biointerf. 27, 365–375.

Kolhe, P., Misra, E., Kannan, R.M., Kannan, S., Lieh-Lai, M., 2003. Drug complexation, *in vitro* release and cellular entry of dendrimers and hyperbranched polymers. Int. J. Pharm. 259, 143–160.

Mallamace, F., Canetta, E., Lombardo, D., Mazziglia, A., Romeo, A., Monsú Scolaro, L., Maino, G., 2002. Scaling properties in the internal structure of dendrimer systems. Physica A 304, 235–243.

Mc Fadden, D.C., Seeber, F., Boothroyd, J.C., 1997. Use of *Toxoplasma gondii* expressing beta-galactosidase for colorimetric assessment of drug activity *in vitro*. Antimicrob. Agents Chemother. 41, 1849–1853.

Mecke, A., Uppuluri, S., Sassanella, T.M., Lee, D.K., Ramamoorthy, A., Baker Jr., J.R., Orr, B.G., Banaszak Holl, M.M., 2004. Direct observation of lipid bilayer disruption by poly(amidoamine) dendrimers. Chem. Phys. Lipids 132, 3–14.

Nichols, B.A., Chiappino, M.L., Pavesio, C.E., 1994. Endocytosis at the micropore of *Toxoplasma gondii*. Parasitol. Res. 80, 91–98.

Petersen, E., Pollak, A., Reiter-Owona, I., 2001. Recent trends in research on congenital toxoplasmosis. Int. J. Parasitol. 31, 115–144.

Robibaro, B., Hoppe, H.C., Yang, M., Coppens, I., Ngô Huân, M., Stedman, T.T., Paprotka, K., Joiner, K.A., 2001. Endocytosis in different lifestiles of protozoan parasitism: role in nutrient uptake with special reference to *Toxoplasma gondii*. Int. J. Parasitology 31, 1343–1353.

Roos, D.S., Donald, R.G., Morrissette, N.S., Moulton, A.L., 1994. Molecular tools for genetic dissection on the protozoan parasite *Toxoplasma gondii*. Meth. Cell Biol. 45, 27–63.

Saliba, K.J., Kiaran, K., 2001. Nutrient acquisition by intracellular apicomplexan parasites: staying in for dinner. Int. J. Parasitol. 31, 1321–1330.

Samuel, B.U., Hearn, B., Mack, D., Wender, P., Rothbard, J., Kirisits, M.J., Mui, E., Wernimont, S., Roberts, C.W., Muench, S.P., Rice, D.W., Prigge, S.T., Law, A.B., McLeod, R., 2003. Delivery of antimicrobials into parasites. PNAS 100 (24), 14281–14286.

Schatten, H., Ris, H., 2004. Three-dimensional imaging of *Toxoplasma gondii*–host cell interactions within the parasitophorous vacuole. Microsc. Microanal. 10 (5), 580–585.

Schwab, J.C., Beckers, C.J., Koiner, K.A., 1994. The parasitophorous vacuole membrane surronding intracellular *Toxoplasma gondii* functions as a molecular sieve. Proc. Natl. Acad. Sci. USA 91, 509–513.

Sinai, A.P., Webster, P., Joiner, K.A., 1997. Association of host cell endoplasmic reticulum and mitochondria with the *Toxoplasma gondii* parasitophorous vacuole membrane: a high affinity interaction. J. Cell Sci. 110, 2117–2128.

Tai, S., Maiti, P.K., Goddard III, W.A., 2005. Dynamics and thermodynamics of water in PAMAM dendrimers at subnanosecond time scales. J. Phys. Chem. B 109, 863–8672.

Tajarobi, F., EL-Sayed, M., Rege, B.R., Pollo, J.E., Ghandehari, H., 2001. Transport of poly-amidoamine dendrimers across Madin–Darby canine kidney cells. Int. J. Pharm. 215, 263–267.

Uppuluri, S., Keinath, S.E., Tomalia, D.A., Dvornic, P.R., 1998. Rheology of dendrimers. I. Newtonian flow behaviour of medium and highly concentrated solutions of polyamidoamine (PAMAM) dendrimers in ethylenediamide (EDA) solvent. Macromolecules 31, 4498–4510.

Uppuluri, S., Morrison, F.A., Dvornic, P.R., 2000. Rheology of dendrimers. 2. Bulk polyamidoamine dendrimers under steady shear, creep and dynamic oscillator. Macromolecules 33, 2551–2560.

Yang, P.H., Sun, X., Chiu, J.F., Sun, H., He, Q.Y., 2005. Transferrin-mediated gold nanoparticles cellular uptake. Bioconjugate Chem. 16, 494–496.

Zhang, Y.W., Halonen, S.K., Ma, Y.F., Wittner, M., Weiss, L.M., 2001. Initial characterization of CST1, a *Toxoplasma gondii* cyst wall glycoprotein. Infect. Immun. 69 (1), 501–507.

Zhang, Z.Y., Smith, B.D., 2000. High generation polycationic dendrimers are unusually effective at disrupting anionic vesicles: membrana bending model. Bioconjugate Chem. 11, 805–814.